Asia Pacific Science Press

*Asia Pacific Journal of Clinical Medical Research*
*ISSN(O):3079-8345*
*ISSN(P):3079-8337*
*Vol. 1 No.3 (2025)*

# Feasibility Study on the Use of Wireless Optogenetic Regulation of PD-L1 Expression to Remodel the Immune Microenvironment of Glioblastoma

**Jiahe Su***

Shanghai Shangde Experimental School, Shanghai, 201315, China

***Corresponding author: Jiahe Su***



**Abstract:** This study is based on wireless optogenetic technology, utilizing the CRY2/CIB1 photosensitive system to achieve spatiotemporal control of PD-L1 expression. In vitro experiments showed that the surface PD-L1 positivity rate of cells increased from 28.6±3.1% to 67.3±5.4% (P<0.001). In animal experiments, the terminal tumor volume in the light exposure group was 450±90 mm3, with a tumor inhibition rate of approximately 49.4% (P<0.001), and the median survival was extended to 32 days (compared to 24 days in the control group, P=0.004). Immunological tests revealed a significant increase in CD8+ T cell infiltration (112±18 vs 52±10 cells/HPF, P<0.01), a 30% decrease in the proportion of Tregs (P<0.05), and an increase in the M1/M2 macrophage ratio to 1.8. The results suggest that the wireless optogenetic system can not only precisely regulate PD-L1 but also remodel the tumor immune microenvironment, providing a new approach for precise immunotherapy of GBM.

**Keywords:** Wireless Optogenetics; Photosensitive System; PD-L1 Expression; Spatiotemporal Control; Tumor Suppression

**Published:** Sept 5, 2025

**DOI:** https://doi.org/10.62177/apjcmr.v1i3.591

## Introduction

Glioblastoma (GBM) is one of the most common malignant gliomas in the central nervous system, characterized by rapid proliferation, infiltrative growth, and high resistance to conventional radiochemotherapy [1]. At present, the standard treatment regimen is surgical resection combined with radiochemotherapy. However, due to the diffuse infiltration of tumor cells at the microscopic level, residual tumor cells are easily left behind. The significant heterogeneity and redundant molecular pathways of GBM lead to a low median survival and survival rate in patients [2]. One of the key factors in the immune suppression mechanisms of GBM is the high expression of programmed death ligand 1 (PD-L1). PD-L1 can bind to the PD-1 receptor on the surface of tumor-infiltrating lymphocytes, triggering an immune inhibitory signaling pathway that leads to the exhaustion of effector T cells, allowing tumor cells to evade immune system clearance [3]. In addition, optogenetics is a cutting-edge technology that uses light-sensitive proteins to achieve spatiotemporal-specific control of cellular activity or gene expression. It has been widely applied in neuroscience, developmental biology, and gene therapy [4]. By introducing specific light-sensitive elements, the expression of target genes can be activated or inhibited under specific wavelengths of light, enabling highly precise regulation of cellular functions.

Based on the above background, this paper employs a wireless optogenetic method, using wireless energy transfer and

a micro light source to remotely and controllably inhibit the expression of PD-L1 in brain tumor sites. Compared with traditional optogenetic methods, wireless optogenetics avoids the trauma and physical restrictions caused by wires, making it more suitable for deep brain tissues and long-term in vivo experiments. This approach is not only technically feasible but also has the potential to break through the current bottleneck in glioblastoma immunotherapy, providing a new direction for theoretical and technical research in creating high-precision immune intervention measures.

# 1.Materials and Methods

## 1.1 Cell and Animal Models

### 1.1.1 Cells

Two human glioblastoma (GBM) cell lines, U87 and LN229 (American Type Culture Collection, ATCC, Manassas, VA, USA) [5], were selected for this study.

The cells were cultured in high-glucose DMEM (Dulbecco's Modified Eagle Medium, Gibco, Thermo Fisher Scientific, Cat# 11965-092, USA) supplemented with 0% fetal bovine serum (FBS, Gibco, Thermo Fisher Scientific, Cat# 10099-141, USA) and 1% penicillin-streptomycin (Gibco, Thermo Fisher Scientific, Cat# 15140-122, USA). The cultures were maintained in a humidified incubator at 37°C with 5% CO2 (Thermo Scientific™ Forma™ Series II Water Jacket CO2 Incubator, Model 3110, USA).

When the cell confluence reached approximately 80%, the cells were digested with 0.25% trypsin-EDTA (Gibco, Thermo Fisher Scientific, Cat# 25200-056, USA). After rinsing with PBS (Phosphate Buffered Saline, HyClone, Cytiva, Cat# SH30256.01, USA), the cells were passaged.

Based on the optogenetic system and light exposure conditions, the cells were divided into the following groups: control group (no light/no vector), empty vector group (transfected with the optogenetic system vector but no light exposure), light exposure group (optogenetic system vector + blue light exposure), and negative control group (empty vector + blue light exposure).

### 1.1.2 Animal Models

Immunodeficient mouse models were established using 6–8-week-old female BALB/c nude mice (SPF grade), which were employed for xenograft glioblastoma (GBM) tumor models. Humanized immune system mouse models were generated using NOD-scid IL2Rγnull (NSG) mice through hematopoietic stem cell transplantation to reconstitute a humanized immune system (hu-PBMCs), enabling evaluation of immune microenvironment modulation. U87 or LN229 cells were resuspended in PBS at a concentration of 1×10^7 cells/mL, and 100 μL of suspension was subcutaneously inoculated into the right axilla of the mice. Each model included four groups: control, empty vector, light stimulation, and negative control (n = 8 per group). Specifically, immunodeficient models were established with 6–8-week-old female BALB/c nude mice (SPF grade, Beijing Vital River Laboratory Animal Technology Co., Ltd., China). Humanized immune system models were constructed with 6–8-week-old female NSG mice (SPF grade, The Jackson Laboratory, Cat# 005557, USA). Human peripheral blood mononuclear cells (PBMCs) for transplantation were obtained from Stemcell Technologies, Vancouver, Canada. U87 or LN229 cells were resuspended in PBS (HyClone, Cytiva, Cat# SH30256.01, USA) at 1×10^7 cells/mL, and 100 μL of the suspension was subcutaneously injected into the right axilla using a microsyringe (Hamilton, 25 μL/100 μL, Model 701/702, USA).

Mice were maintained in an IVC (individually ventilated cage) system (Tecniplast, Italy, Model GM500) under controlled temperature (22 ± 2 °C), humidity (50 ± 10% RH), and a 12-h light/dark cycle, with free access to standard laboratory chow and water.

## 1.2 Optogenetic System Design

### 1.2.1 Light-Controlled Genetic Elements

To achieve reversible and spatially specific control of PD-L1 expression, this study constructed a light-controlled transcriptional regulation element based on the CRY2/CIB1 light-induced dimerization system. Under blue light irradiation (λ≈470 nm), CRY2 dimerizes with CIB1, recruiting the bound transcriptional activator (VP64) to the PD-L1 promoter region to enhance the transcription of the PD-L1 gene. Lentiviral vectors pLenti-EF1α (Addgene, USA) were used to package the CRY2-transcription factor fusion protein and the CIB1-DNA binding domain fusion protein, respectively, and a light-sensitive

regulatory element was introduced upstream of the PD-L1 promoter. A blue light LED light source (470 nm, M470L4, Thorlabs, USA) was used in conjunction with a fiber optic coupling system (Doric Lenses, Canada) to achieve localized light exposure both in vitro and in vivo. The light response characteristics and PD-L1 expression changes were verified by transient transfection in HEK-293T cells (ATCC, USA).

### 1.2.2 Gene Delivery

Transfection was performed using Lipofectamine™ 3000 (Thermo Fisher Scientific, USA), and PD-L1 baseline levels were assessed 48 h post-transfection. For in vivo delivery, lentiviruses carrying the optogenetic elements (1×10^8 TU/mL, Hanbio Biotechnology, China) were intratumorally injected at a volume of 50 μL every other day for a total of three injections.

## 1.3 Wireless Light Delivery Device

### 1.3.1Wireless Light Delivery Device Construction

The main structure of the device is composed of a miniaturized wearable LED module, a wireless battery, and a Bluetooth control unit. The total weight is 1.5 g, which is designed to be fixed on the back of a mouse without affecting its free movement; the size is 10×8×5 mm. A lightweight silicone sleeve and medical tape are used for fixation to ensure that the light is accurately targeted at the tumor site.

### 1.3.2 Optical Parameters

Wavelength (λ): 470 ± 5 nm (blue light); power density: 5–10 mW/cm²; adjustable emission modes: continuous or pulsed light (10 Hz, 50% duty cycle); the heat dissipation system consisted of an aluminum substrate combined with miniature cooling fins to prevent the skin temperature of the animals from rising above 2 ℃.

### 1.3.3 Control Methods

The lighting duration, power, and mode were remotely controlled via Bluetooth 5.0. The light was set for 30 minutes daily for 14 consecutive days. In control mice without the carrier, 7 consecutive days of illumination caused no skin burns or restricted activity.

## 1.4 Statistical Analysis

Western blot: Total protein was extracted using RIPA lysis buffer, separated by SDS-PAGE, and transferred onto PVDF membranes. The membranes were incubated with anti–PD-L1 (1:1000, CST) and anti–GAPDH (1:5000, Abcam) antibodies, followed by ECL detection. Band intensity was quantified using ImageJ software.

qPCR: Total RNA was extracted with TRIzol reagent, reverse-transcribed into cDNA using the PrimeScript RT kit (Takara), and subjected to quantitative PCR with SYBR Green for detection of PD-L1 mRNA expression, with β-actin as the internal control.

Flow cytometry: Cells were labeled with PD-L1–FITC antibody, and surface PD-L1 positivity was analyzed on a FACSCalibur flow cytometer. Immunohistochemistry (IHC): Paraffin-embedded tumor sections were incubated with antibodies against CD8, CD4, F4/80, and Foxp3, followed by DAB chromogenic staining. Images were acquired under a light microscope, and infiltrating immune cells were quantified.

Single-cell suspensions were stained with immune markers (CD45, CD8, CD4, CD11b, etc.) and analyzed to determine the proportions of different immune cell subsets.

Tumor volumes were measured every 3 days using a caliper, and calculated according to the formula:

$$V=\frac{1}{2}\times\text{length}\times(\text{width})^2 \tag{1}$$

Tumor Growth Inhibition (TGI):

$$V=\frac{1}{2}\times\text{length}\times 100 \tag{2}$$

Kaplan-Meier survival curves were used, and differences between groups were assessed using the log-rank test. All experiments were repeated at least three times. Data are presented as mean ± standard deviation (SD). One-way analysis of variance (ANOVA) followed by Tukey's post hoc test was used for comparisons between groups. $P<0.05$ was considered statistically significant.

# 2.Results

## 2.1 Regulation of PD-L1 Expression

HEK-293T, U87, and LN229 cells were transfected with the optogenetic vector and subjected to blue light illumination (470 nm, 5 mW/cm², 30 min). PD-L1 protein and mRNA levels were measured by Western blot and qPCR, respectively, as shown in Table 1. *P<0.05, **P<0.01, **P<0.001. The results indicated that PD-L1 expression remained at baseline levels in the control and empty vector groups. In the illuminated group, PD-L1 protein expression was significantly upregulated (U87: 2.1 ± 0.3-fold; LN229: 1.8 ± 0.2-fold, P<0.01), with mRNA levels showing a corresponding increase. No significant changes were observed in the negative control group. Flow cytometry further confirmed differences in cell surface PD-L1 positivity: the illuminated group exhibited a positive rate of 67.3 ± 5.4%, significantly higher than the control group (28.6 ± 3.1%, P<0.001), suggesting that the optogenetic system can enhance PD-L1 expression under spatially specific conditions.

*Tab.1 Results of Light-Controlled Regulation of PD-L1 Expression in Different Cell Lines*

| Cell lines | Group | PD-L1 protein expression | PD-L1 mRNA expression | PD-L1 positivity rate |
|---|---|---|---|---|
| HEK-293T | Control Group | 1.0±0.1 | 1.0±0.1 | 15.2±2.4 |
| | Empty vector group | 1.1±0.1 | 1.0±0.1 | 16.7±2.1 |
| | Light group | 1.5±0.2* | 1.6±0.2* | 32.8±4.3* |
| | Negative control group | 1.0±0.1 | 1.1±0.1 | 14.9±2.7 |
| U87 | Control Group | 1.0±0.1 | 1.0±0.1 | 28.6±3.1 |
| | Empty vector group | 1.0±0.1 | 1.1±0.1 | 29.4±3.0 |
| | Light group | 2.1±0.3** | 2.0±0.3** | 67.3±5.4*** |
| | Negative control group | 1.1±0.1 | 1.1±0.2 | 27.8±2.9 |
| LN229 | Control Group | 1.0±0.1 | 1.0±0.1 | 22.5±2.6 |
| | Empty vector group | 1.0±0.1 | 1.0±0.1 | 23.1±2.4 |
| | Light group | 1.8±0.2** | 1.7±0.2** | 54.7±4.6*** |
| | Negative control group | 1.1±0.1 | 1.0±0.2 | 22.0±2.5 |

## 2.2 Applicability and Safety

In the BALB/c nude mouse GBM xenograft model, animals wearing the wireless light delivery device exhibited normal free movement, and their weight curves showed no significant differences compared to the group without the device. During light exposure, the skin temperature on the back of the mice increased by no more than 1.8°C, which is within the safety standard. The results in Table 2 show that in the safety pre-experiment (n=5), continuous light exposure for 7 days (30 min/d) did not result in skin damage or restricted movement. Histological sections revealed no significant inflammatory response, confirming the feasibility of long-term application of the device.

*Tab.2 Safety Evaluation of the Wireless Light Delivery Device in BALB/c Nude Mouse GBM Model*

| Indicator | Control Group (No Device, n=5) | Device Group (With Device, n=5) | Light Safety Group (With Device, n=5, Continuous 7 days, 30 min/d) | Statistical Difference |
|---|---|---|---|---|
| Weight Change (g) | Initial: 18.4 ± 1.2<br>7 days: 19.1 ± 1.3 | Initial: 18.6±1.1<br>7 days: 19.0±1.4 | Initial: 18.7±1.0<br>7 days: 19.2±1.2 | NS(P>0.05) |
| Weight Change Rate (%) | +3.8±1.2 | +2.7±1.5 | +2.9±1.3 | NS |
| Back Skin Temperature Increase (°C) | 0.2±0.1 | 0.3±0.1 | 1.8±0.2 (During Light Exposure) | < Safety Threshold 2°C |
| Skin Damage | None observed | None observed | None observed | - |

| Indicator | Control Group (No Device, n=5) | Device Group (With Device, n=5) | Light Safety Group (With Device, n=5, Continuous 7 days, 30 min/d) | Statistical Difference |
|---|---|---|---|---|
| Activity Status | Normal, free movement | Normal, free movement | Normal, free movement | - |
| Histological Examination (HE Staining) | Normal skin and subcutaneous tissue structure | Normal | No significant inflammation or necrosis | - |

## 2.3 Effect of Optogenetic Modulation on Tumor Growth

In the U87 and LN229 xenograft tumor models, tumor volume was monitored every 3 days. Table 3 shows that tumors in the control and empty vector groups grew rapidly, reaching volumes of 890 ± 120 mm³ and 865 ± 105 mm³ on day 14, respectively. Tumor growth in the illumination group slowed significantly, reaching a terminal volume of only 450 ± 90 mm³, with a tumor inhibition rate (TGI) of approximately 49.4% ($P < 0.001$). There was no significant difference between the negative and control groups ($P > 0.05$). Survival analysis showed that the median survival in the illumination group was approximately 35% longer than in the control group (24 days in the control group vs. 32 days in the illumination group, $P = 0.004$), suggesting that optogenetic modulation has an anti-tumor effect in vivo.

*Tab.3 Anti-tumor effects of optogenetic regulation on U87 and LN229 transplanted tumor models*

| Indicator | Control Group | Empty vector group | Light group | Negative control group | P value |
|---|---|---|---|---|---|
| End-stage tumor volume U87($mm^3$) | 890±120 | 865±105 | 450±90 | 880±115 | P<0.001 |
| End-stage tumor volume LN229($mm^3$) | 910±130 | 885±125 | 470±85 | 900±120 | P<0.001 |
| Tumor inhibition rate (TGI,%) | 0% | 2.8% | 49.4% | 1.1% | P>0.05 |
| Median survival time (d) | 24 | 25 | 32 | 23 | P=0.004 |
| Extended survival rate (%) | 0% | 4.2% | 35% | -4.2%% | P=0.004 |

## 2.4 Changes in the Tumor Immune Microenvironment

As shown in Table 4, the light exposure group exhibited a significant increase in CD8+ T cell infiltration in the tumor tissue, with 112±18 cells/HPF compared to 52±10 cells/HPF in the control group, representing more than a twofold increase (P<0.01). The number of CD4+ T cells also increased (P<0.05). The proportion of Foxp3+ Treg cells decreased (P<0.05), indicating a partial reversal of the immunosuppressive state. F4/80+ macrophage infiltration in the light exposure group showed an increase in the M1 phenotype and a decrease in the M2 phenotype (immunostaining ratio M1/M2≈1.8), suggesting that optogenetic regulation may promote antitumor immune polarization.

Flow cytometry analysis of single-cell suspensions revealed that the proportion of CD8+ T cells in the light exposure group increased to 28.6±3.2%, significantly higher than the control group (15.2±2.1%) (P<0.001). The proportion of CD4+ T cells also increased (P<0.05). The proportion of Tregs (CD4+CD25+Foxp3+) decreased by 30% (P<0.05). Among myeloid cells (CD11b+), the proportion of M1 phenotype increased, indicating a shift towards an immunologically activated tumor microenvironment.

*Tab.4 Effects of Optogenetic Regulation on the Tumor Immune Microenvironment in GBM Xenograft Models*

| Indicator | Control Group | Light Exposure Group | P-value |
|---|---|---|---|
| CD8+ T cell infiltration (cells/HPF, IHC) | 52±10 | 112±18 | P<0.01 |
| CD4+ T cell infiltration (cells/HPF, IHC) | 68±12 | 92±15 | P<0.05 |
| Foxp3+ Treg infiltration (cells/HPF, IHC) | 41±9 | 28±7 | P<0.05 |
| F4/80+ Macrophages (M1/M2 ratio, IHC) | 0.9±0.2 | 1.8±0.3 | P<0.01 |
| CD8+ T cell proportion (% of CD45+, Flow Cytometry) | 15.2±2.1% | 28.6±3.2% | P<0.001 |

| Indicator | Control Group | Light Exposure Group | P-value |
|---|---|---|---|
| CD4+ T cell proportion (% of CD45+, Flow Cytometry) | 22.5±3.0% | 28.1±3.5% | P<0.05 |
| Treg proportion (CD4+CD25+Foxp3+, % of CD4+) | 12.0±1.8% | 8.4±1.5% | P<0.05 |
| Myeloid cells (CD11b+, % of CD45+, Flow Cytometry) | 18.5±2.6% | 19.2±2.8% | NS |
| M1 macrophage proportion (% of CD11b+, Flow Cytometry) | 34.2±4.1% | 52.5±5.0% | P<0.01 |
| M2 macrophage proportion (% of CD11b+, Flow Cytometry) | 38.5±4.3% | 29.1±3.6% | P<0.05 |

### 2.5 Mechanistic Hypotheses

The dual mechanisms of optogenetic regulation of the tumor immune microenvironment are shown in Figure 1. The optogenetic system upregulates PD-L1 expression on the surface of tumor cells, which initially may promote the activation of the PD-L1/PD-1 axis. However, long-term local blue light stimulation may counteract immune evasion through immune remodeling effects (such as enhanced CD8+ T cell infiltration, Treg suppression, and macrophage polarization), thereby leading to an overall antitumor effect. This phenomenon suggests that optogenetic regulation can not only be used for studying PD-L1 function but may also serve as an experimental basis for precise spatiotemporal immunotherapy strategies.

*Fig.1 Optogenetic regulation of PD-L1 and immune remodeling*

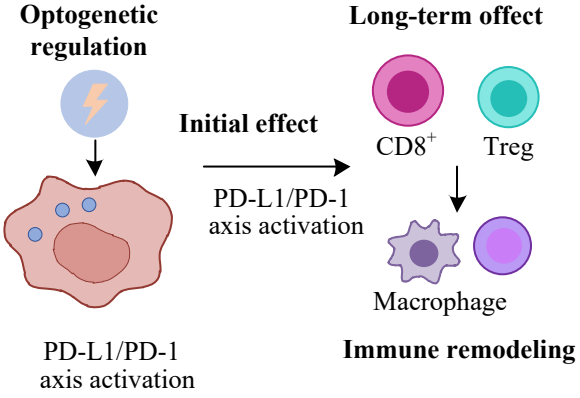


## 3.Conclusion

This study has confirmed that the wireless optogenetic system can effectively regulate PD-L1 expression and improve the immune environment in GBM both in vitro and in vivo. In vitro experiments showed that blue light stimulation significantly enhanced PD-L1 levels on the surface of tumor cells. In the xenograft tumor model, the system achieved marked tumor suppression (terminal volume 450±90 mm³, TGI=49.4%) and significantly extended the median survival of mice to 32 days. Immunological analysis revealed that in the light exposure group, CD8+ T cell infiltration doubled (112±18 vs 52±10 cells/HPF), the proportion of Foxp3+ Tregs decreased (8.4±1.5% vs 12.0±1.8%), and the proportion of M1 macrophages increased (52.5±5.0% vs 34.2±4.1%). These results indicate that optogenetic regulation not only elucidates the function of PD-L1 but also has the potential to reverse immune suppression and promote immune activation, thereby exerting antitumor effects. Wireless optogenetics provides a feasible experimental basis for precise, spatiotemporally controlled immunotherapy strategies for GBM and holds potential for clinical translation.

## Funding

no

## Conflict of Interests

The authors declare that there is no conflict of interest regarding the publication of this paper.

## Reference

[1] Makowska, M., Smolarz, B., & Romanowicz, H. (2023). MicroRNAs (miRNAs) in glioblastoma multiforme (GBM)—

recent literature review. International Journal of Molecular Sciences, 24(4), 3521.

[2] Tang, H., Wang, H., Fang, Y., Li, J., Zhang, L., Chen, K., ... & Li, Y. (2023). Neoadjuvant chemoradiotherapy versus neoadjuvant chemotherapy followed by minimally invasive esophagectomy for locally advanced esophageal squamous cell carcinoma: A prospective multicenter randomized clinical trial. Annals of Oncology, 34(2), 163–172.

[3] Lin, H., Liu, C., Hu, A., Li, L., Wang, X., Zhang, L., ... & Wang, Y. (2024). Understanding the immunosuppressive microenvironment of glioma: Mechanistic insights and clinical perspectives. Journal of Hematology & Oncology, 17(1), 31.

[4] Armbruster, A., Mohamed, A. M. E., Phan, H. T., Gogolla, N., & Diester, I. (2024). Lighting the way: Recent developments and applications in molecular optogenetics. Current Opinion in Biotechnology, 87, 103126.

[5] Bhardwaj, S., Sanjay, & Yadav, A. K. (2025). Higher isoform of hnRNPA1 confers temozolomide resistance in U87MG & LN229 glioma cells. Journal of Neuro-Oncology, 171(1), 47–63.